Journal of Electrical and Computer Engineering Innovations
(JECEI)
Journal homepage: http://www.jecei.sru.ac.ir

Research paper

A General Approach for Operational Bandwidth Extension in Spherical Microphone Array

M. Kalantari*, M. Mohammadpour Tuyserkani, S.H. Amiri

Faculty of Computer Engineering, Shahid Rajaee Teacher Training University, Tehran, Iran.

Article Info

Article History:
Received 06 October 2021
Reviewed 23 November 2021
Revised 06 December 2021
Accepted 03 February 2022

Keywords:
Spherical microphone arrays
Aliasing
Beamforming
Operational bandwidth

Corresponding Author's Email Address: *mkalantari@sru.ac.ir*

Abstract

Background and Objectives: Operating frequency range of a microphone array is limited by the array configuration. Spatial aliasing occurs at frequencies considered to be out of the microphone array operating range that leads to side-lobes in the array beam pattern and consequently degrades the performance of the microphone array. In this paper, a general approach for increasing the operational bandwidth of the spherical microphone array without physical changes to the microphone array is proposed.

Methods: Recently, Alon and Rafaely proposed a beamforming method with aliasing cancellation and formulated it for some well-known beamformers such as maximum directivity (MD), maximum white noise gain (WNG), and minimum variance distortionless response (MVDR) which have been called MDAC, MGAC, MVDR-AC beamformer respectively. In this paper, we derive MDAC method from different point of view. Then, based on our perspective, we propose a new method that is easily applicable for any beamforming algorithms.

Results: Comparing with MDAC and MGAC beamformers, performance measures for our approach show improvement in directivity index (DI) and white noise gain (WNG) by nearly 19% and 15% respectively.

Conclusion: Aliasing and, in consequence, unwanted side lobe formation is the main factor in spherical microphone arrays operational bandwidth determination. Most of the methods previously presented to reduce aliasing demanded physical changes in the array structure which comes at a cost. In this paper we propose a new method based on Alon and Rafaely's approach via designing a constrained optimization problem using orthogonality property of spherical harmonics, to achieve better performance.

Introduction

Spherical microphone arrays are a type of microphone arrays that have a spherical array structure in which microphones are placed on the surface of a sphere. This kind of microphone arrays has been an interesting field of study for the past decade. Because of their symmetry they can steer the beam pattern over any desired direction in the space [1].

One of the main concepts central to spherical microphone arrays is its operational bandwidth [2]-[9]. The operational bandwidth of the spherical microphone arrays is determined by their lower and upper frequency limits [10], [11]. The lower frequency limit is bounded by some factors such as sensor noise and the upper frequency limit is bounded by spatial aliasing [8], [12]. In fact, analyzing the array bandwidth limitations by

decomposing the sound field into spherical harmonics shows that with the increase of the frequency, the sound pressure function of the sound field around the sphere will be of a higher order [10], [13]. In many cases this order is higher than the array's maximum order, which is determined by the number of microphones that leads to spatial aliasing [14], [15].

Spatial aliasing and consequently unwanted side-lobe formation is the main cause of performance degradation of spherical microphone arrays at high frequencies [16], [17]. Some solutions have been presented for reducing aliasing effects [18]-[20], but they can only perform well in a sound field with certain characteristics [21], [22]. Other methods for increasing arrays performance in high frequencies tend to minimize side-lobe levels [23]. These methods include increasing the number of microphones in the array, using other types of directional microphones, or using microphones with wider surface [7], [24]-[26], [10], [19], [27], [28]. All the methods mentioned above need to make physical changes in the array structure that comes with a cost in many cases.

Recently Alon and Rafaely proposed a new spherical microphone array beamforming with an aliasing model for describing high sound field orders, aliased into the lower array orders. For that, they include the effect of spatial aliasing in the definition of desired objective, such as directivity factor, and develop a new version of beamformers with aliasing cancellation capabilities. Their method was found to be valuable for injecting aliasing cancellation capability to some of the well-known beamformers such as maximum directivity (MD) beamformer, after which called maximum directivity beamformer with aliasing cancellation (MDAC). This new beamformer achieves higher directivity index (DI) with a narrower main lobe and lower side lobes, compared with standard MD beamformer. This method was also used to develop maximum white noise gain with aliasing cancellation (MGAC), and minimum variance distortionless response with aliasing cancellation (MVDR-AC) beamformers [1].

In this paper we aim to look at the method presented by Alon and Rafaely from a different point of view. The main contribution of this work is to design a constrained optimization problem with some appropriate constraints to find the closest signal to the desired unaliased signal. These constraints are attained by using the orthogonality property of spherical harmonics. Then this estimation of unaliased signal can be used in beamforming process using ordinary beamforming coefficient of a high order beamfomer.

This paper is organized as follows. The second section reviews the spherical array processing fundamentals. The third section presents the proposed method for aliasing cancellation beamforming. Simulation results and comparisons with the rival method are presented in the fourth section, and the end section concludes the paper.

Spherical Array Processing

This section shortly explains the theory of spherical microphone array processing [16], [29]. The formulation provided in this section will be utilized in the third section to develop the proposed beamformer.

A. Spherical Array Processing

Consider a sound field composed of multiple "single frequency plane wave" each with amplitude density denoted by $a(k,\theta_k,\phi_k)$ arriving from direction (θ_k,ϕ_k) with a wave vector $\tilde{\mathbf{k}}=-\mathbf{k}=(k,\theta_k,\phi_k)$ and wave number k. The sound pressure at $\mathbf{r}=(r,\theta,\phi)$ due to this sound field can be written as follows [16]

$$p(k,r,\theta,\phi)=\sum_{n=0}^{\infty}\sum_{m=-n}^{n}p_{nm}(k,r)Y_n^m(\theta,\phi) \quad (1)$$

where $p_{nm}(k,r)$ are the spherical harmonic coefficients of the sound pressure, and $Y_n^m(\theta,\phi)$ are the spherical harmonics. The relation between the pressure on the sphere and the amplitude of the plane waves composing the sound field in the spherical harmonic domain is

$$p_{nm}(k,r)=b_n(kr)a_{nm}(k) \quad (2)$$

where $a_{nm}(k)$ is the spherical Fourier transform of $a(k,\theta_k,\phi_k)$, i.e.,

$$a_{nm}(k)=\int_0^{2\pi}\int_0^{\pi}a(k,\theta_k,\phi_k)[Y_n^m(\theta_k,\phi_k)]^*\sin\theta_k d\theta_k d\phi_k \quad (3)$$

and $b_n(kr)$ defines the projection of the sound field onto the sphere surface. The expression for $b_n(kr)$ depends on the array configuration. For example, in the case of a single open sphere, we have

$$b_n(kr)=4\pi i^n j_n(kr) \quad (4)$$

where $j_n(x)$, is the spherical Bessel function of the first kind.

If the pressure function is order-limited, meaning that $p_{nm}(k,r)=0\ \forall n>N$, then we can represent the function by a finite number of spherical harmonics, so we have

$$p(k,r,\theta,\phi)=\sum_{n=0}^{N}\sum_{m=-n}^{n}p_{nm}(k,r)Y_n^m(\theta,\phi) \quad (5)$$

Equation (1) is, in fact, the inverse spherical Fourier transform of the pressure function [14]. So, we have

$$p_{nm}=\int_0^{2\pi}\int_0^{\pi}p(\theta,\phi)[Y_n^m(\theta,\phi)]^*\sin\theta d\theta d\phi \quad (6)$$

which is the spherical Fourier transform of $p(\theta,\phi)$. For the sake of simplicity, parameters k,r have been omitted.

According to the Cubature method, it can be possible to compute the multiple integrations of a given function using a summation over sample of the function [29]. So,

$$p_{nm} \approx \sum_{q=1}^{Q} \alpha_q \, p(\theta,\phi)[Y_n^m(\theta,\phi)]^* = \hat{p}_{nm} \tag{7}$$

where Q, is the total number of samples and α_q is the sampling weight whose value depends on the sampling scheme. For order-limited function, the approximation becomes equality, given a sufficiently large Q. In this case, $p(\theta,\phi)$ can be reconstructed perfectly on the sphere using the inverse spherical Fourier transform. But, in the case of p_{nm} of infinite order, perfect reconstruction is not possible due to aliasing.

Several sampling methods, such as equal-angle, Gaussian, and uniform sampling, have been previously presented [16], for which the sampling weight α_q and sampling points (θ_q,ϕ_q) have been derived such that (6) is maintained with equality for order-limited functions.

Due to some constraints, we may want to use any arbitrary given sampling set. So, assume that the samples of the function, $p(\theta_q,\phi_q)$, are given, together with the positions of the samples, (θ_q,ϕ_q), for $q = 1,\dots,Q$. Using (5) we have

$$p(\theta_q,\phi_q) = \sum_{n=0}^{N}\sum_{m=-n}^{n} p_{nm} Y_n^m(\theta_q,\phi_q), \quad 1 \le q \le Q, \tag{8}$$

This equation can be written in matrix forms as

$$\mathbf{p} = \mathbf{Y}\mathbf{p_{nm}} \tag{9}$$

where column vectors $\mathbf{p}$ of length Q and $\mathbf{p_{nm}}$ of length $(N+1)^2$ are defined as

$$\mathbf{p} = \left[p(\theta_1,\phi_1), p(\theta_2,\phi_2), \dots, p(\theta_Q,\phi_Q)\right]^T \tag{10}$$

and

$$\mathbf{p_{nm}} = \left[p_{00}, p_{1(-1)}, p_{10}, p_{11}, \dots, p_{NN}\right]^T \tag{11}$$

and the matrix $\mathbf{Y}$ of dimensions $Q \times (N+1)^2$ is shown in (12),

$$\mathbf{Y} = \begin{bmatrix} Y_0^0(\theta_1,\phi_1) & Y_1^{-1}(\theta_1,\phi_1) & Y_1^0(\theta_1,\phi_1) & Y_1^1(\theta_1,\phi_1) & \dots & Y_N^N(\theta_1,\phi_1) \\ Y_0^0(\theta_2,\phi_2) & Y_1^{-1}(\theta_2,\phi_2) & Y_1^0(\theta_2,\phi_2) & Y_1^1(\theta_2,\phi_2) & \dots & Y_N^N(\theta_2,\phi_2) \\ \vdots & \vdots & \vdots & \vdots & \ddots & \vdots \\ Y_0^0(\theta_Q,\phi_Q) & Y_1^{-1}(\theta_Q,\phi_Q) & Y_1^0(\theta_Q,\phi_Q) & Y_1^1(\theta_Q,\phi_Q) & \dots & Y_N^N(\theta_Q,\phi_Q) \end{bmatrix} \tag{12}$$

Equation (9) is called inverse discrete spherical Fourier transform. Also,

$$\mathbf{p_{nm}} = \mathbf{Y}^{\dagger}\mathbf{p} \tag{13}$$

is called discrete spherical Fourier transform, where $\mathbf{Y}^{\dagger} = (\mathbf{Y}^H\mathbf{Y})^{-1}\mathbf{Y}^H$ is the pseudo-inverse of $\mathbf{Y}$. This equation can be written in the following form

$$p_{nm} = \sum_{q=1}^{Q} \alpha_q^{nm} \, p(\theta_q,\phi_q) \tag{14}$$

where the sampling weights, α_q^{nm}, are the elements of matrices $\mathbf{Y}^{\dagger}$, having a row index given by (n^2+n+m) and a column index is given by q.

B. Spatial Aliasing

As we have already mentioned, sampling of order-limited functions on the sphere with an appropriate sampling scheme should lead to an exact and aliasing-free computation of the spherical harmonic coefficient. But for non-order-limited functions, errors may occur due to spatial aliasing. For analyzing and describing these errors, we can rewrite (7) as follows [24]:

$$\begin{aligned} \hat{p}_{nm} &= \sum_{q=1}^{Q} \alpha_q^{nm} \sum_{n'=0}^{\infty}\sum_{m'=-n'}^{n'} p_{n'm'} Y_{n'}^{m'}(\theta_q,\phi_q) \\ &= \sum_{n'=0}^{\infty}\sum_{m'=-n'}^{n'} \left[\sum_{q=1}^{Q} \alpha_q^{nm} Y_{n'}^{m'}(\theta_q,\phi_q)\right] p_{n'm'} \\ &= \sum_{n'=0}^{\infty}\sum_{m'=-n'}^{n'} \epsilon_{nm}^{n'm'} p_{n'm'}, \end{aligned} \tag{15}$$

where

$$\epsilon_{nm}^{n'm'} = \sum_{q=1}^{Q} \alpha_q^{nm} Y_{n'}^{m'}(\theta_q,\phi_q) \tag{16}$$

In an ideal, aliasing-free sampling, $\epsilon_{nm}^{n'm'}$ equals one for $(n,m) = (n',m')$ and zero elsewhere. If we assume that the spherical harmonic coefficients of the original function before sampling, $p_{n'm'}$, is order-limited but to very high order denoted by $\tilde{N}$, we can represent (14) in a matrix form as follows

$$\hat{\mathbf{p}}_{\mathbf{nm}} = \mathbf{E}\tilde{\mathbf{p}}_{\mathbf{nm}} \tag{17}$$

where $\hat{\mathbf{p}}_{\mathbf{nm}}$ of length $(N+1)^2$ holds the approximated spherical harmonic coefficients $\hat{p}_{nm}$, $\tilde{\mathbf{p}}_{\mathbf{nm}}$ of length $(\tilde{N}+1)^2$ holds the spherical harmonic coefficients p_{nm} of the original function, with $\tilde{N} \ge N$, and matrix $\mathbf{E}$ of dimensions $(N+1)^2 \times (\tilde{N}+1)^2$, having elements $\epsilon_{nm}^{n'm'}$ with row index (n^2+n+m) and column index $(n'^2+n'+m')$, called aliasing matrix. Matrix $\mathbf{E}$ can be written as

$$\mathbf{E} = \mathbf{Y}^{\dagger}\tilde{\mathbf{Y}} \tag{18}$$

where matrix $\mathbf{Y}$ of dimensions $Q \times (N+1)^2$ has been defined in (12) and matrix $\tilde{\mathbf{Y}}$ of dimensions $Q \times (\tilde{N}+1)^2$, holding the values of $Y_{n'}^{m'}(\theta_q,\phi_q)$ as in (16).

C. Spherical Array Beamforming

Array equations or beamforming equations is as follows [29]

$$y = \int_0^{2\pi}\int_0^{\pi} w^*(k,\theta,\phi)p(k,r,\theta,\phi)\sin\theta d\theta d\phi = \sum_{n=0}^{\infty}\sum_{m=-n}^{n} w_{nm}^*(k)p_{nm}(k,r) \quad (19)$$

where $w^*(k,\theta,\phi)$, is the beamforming coefficients. The standard discrete form of beamforming in the space domain is

$$y = \mathbf{w^H p} \quad (20)$$

where $\mathbf{p}$ is as (10) with a little modification in notation

$$\mathbf{p} = \left[p_1(k), p_2(k), \dots, p_Q(k)\right]^T \quad (21)$$

with $p_q(k) = p(k,r,\theta_q,\phi_q)$, $q = 1,\dots,Q$, and $\mathbf{w}$ is the $Q \times 1$ weight vector as follows

$$\mathbf{w} = \left[w_1(k), w_2(k), \dots, w_Q(k)\right]^T \quad (22)$$

Assuming $w_{nm} = 0\ \forall n > N$, the discrete form of beamforming in spherical harmonic domain is as

$$y = \mathbf{w_{nm}^H p_{nm}} \quad (23)$$

where the $(N+1)^2 \times 1$ vector $\mathbf{w_{nm}}$ is given by

$$\mathbf{w_{nm}} = \left[w_{00}(k), w_{1(-1)}(k), w_{10}(k), w_{11}(k)\ \dots, w_{NN}(k)\right]^T, \quad (24)$$

and the $(N+1)^2 \times 1$ vector $\mathbf{p_{nm}}$ is given by

$$\mathbf{p_{nm}} = \left[p_{00}(k,r), p_{1(-1)}(k,r), p_{10}(k,r), \dots, p_{NN}(k,r)\right]^T \quad (25)$$

In these equations $p_{nm}(k)$ and $w_{nm}(k)$ are the spherical Fourier transform of $p(k,r,\theta,\phi)$ and $w(k,\theta,\phi)$ respectively and N is called the effective order of the array.

Array output due to a unit-amplitude plane-wave sound field or array beam pattern is defined as

$$y = \mathbf{w_{nm}^H v_{nm}} \quad (26)$$

where $\mathbf{v_{nm}}$, is a $(N+1)^2 \times 1$ column vector as

$$\mathbf{v_{nm}} = \left[v_{00}(k,r), v_{1(-1)}(k,r), v_{10}(k,r), \dots, v_{NN}(k,r)\right]^T \quad (27)$$

with v_{nm} represents the array input due to the plane wave sound field. Since for unit amplitude plane wave we have [29]

$$a_{nm}(k) = \left[Y_n^m(\theta_k,\phi_k)\right]^* \quad (28)$$

according to (2) we have

$$v_{nm}(k,r) = b_n(kr)\left[Y_n^m(\theta_k,\phi_k)\right]^* \quad (29)$$

where (θ_k,ϕ_k), is the arrival direction of the plane wave.

Using a different set of beamforming coefficients, different beam patterns can be designed. For instance, axis-symmetric beamformers with $w_{nm}^*(k) = \frac{d_n(k)}{b_n(kr)}Y_n^m(\theta_l,\phi_l)$ [29], of which two famous beamformers, namely the maximum directivity (MD) beamformer and the maximum white noise gain (WNG) beamformer described in the sequel. Note that the beamformer coefficients are function of look direction which denoted by (θ_l,ϕ_l) in the above relation.

- **Maximum Directivity Beamformer**

The directivity factor (DF) is the ratio between the array response in the look direction and the average response across all directions and is defined mathematically as follows

$$\mathrm{DF} = \frac{|y(\theta_l,\phi_l)|^2}{\frac{1}{4\pi}\int_0^{2\pi}\int_0^{\pi}|y(\theta,\phi)|^2\sin\theta d\theta d\phi} = \frac{\mathbf{w_{nm}^H A w_{nm}}}{\mathbf{w_{nm}^H B_D w_{nm}}}$$
$$\mathbf{A} = \mathbf{v_{nm}}\mathbf{v_{nm}}^{\mathrm{H}} \quad (30)$$
$$\mathbf{B_D} = \frac{1}{4\pi}diag(|b_0|^2,|b_1|^2,|b_1|^2,\dots,|b_N|^2)$$
$$\mathbf{v_{nm}} = \left[v_{00}, v_{1(-1)}, v_{10}, v_{11}, \dots, v_{NN}\right]^T$$

The explicit dependency of $b_n(kr)$ on kr has been omitted for notation simplicity. Note that in (30) $\mathbf{v_{nm}}$ is the unit-amplitude plane wave arriving from look direction.

The maximum directivity (MD) beamformer is designed to satisfy

$$\underset{\mathbf{w_{nm}}}{\text{minimize}}\ \mathbf{w_{nm}^H B_D w_{nm}} \quad \text{subject to } \mathbf{w_{nm}^H v_{nm}} = 1 \quad (31)$$

Solving the above optimization problem leads to the following beamforming coefficients

$$\mathbf{w_{nm}^{MD^H}} = \frac{\mathbf{v_{nm}^H B_D^{-1}}}{\mathbf{v_{nm}^H B_D^{-1} v_{nm}}} \quad (32)$$

or equivalently

$$w_{nm}^*(k) = \frac{4\pi}{(N+1)^2}\frac{1}{b_n(kr)}Y_n^m(\theta_l,\phi_l) \quad (33)$$

which is an axis-symmetric beamformer with $d_n(k) = \frac{4\pi}{(N+1)^2}$.

- **Maximum WNG Beamformer**

WNG is a general measure for array robustness which is defined as the improvement in SNR at the array output compared to the array input. Mathematically,

$$\mathrm{WNG} = \frac{\mathbf{w_{nm}^H A w_{nm}}}{\mathbf{w_{nm}^H B_G w_{nm}}}$$
$$\mathbf{A} = \mathbf{v_{nm}}\mathbf{v_{nm}^H} \quad (34)$$
$$\mathbf{B_G} = \mathbf{Y}^{\dagger}\mathbf{Y}^{\dagger^H}$$

The maximum WNG beamformer (MG) is designed to satisfy the problem below

$$\begin{aligned} &\underset{\mathbf{w_{nm}}}{\text{minimize}}\ \mathbf{w_{nm}^H B_G\, w_{nm}} \\ &\text{subject to } \mathbf{w_{nm}^H v_{nm}} = 1 \end{aligned} \tag{35}$$

Solving the above optimization problem leads to the following beamforming coefficients

$$\mathbf{w_{nm}^{MG^H}} = \frac{\mathbf{v_{nm}^H B_G^{-1}}}{\mathbf{v_{nm}^H B_G^{-1} v_{nm}}} \tag{36}$$

For uniform or nearly uniform sampling scheme, this leads to

$$w_{nm}^*(k) = \frac{b_n^*(kr)Y_n^m(\theta_l,\phi_l)}{\sum_{n=0}^{N}\frac{2n+1}{4\pi}|b_n(kr)|^2} \tag{37}$$

which is an axis-symmetric beamformer with $d_n(k) = \frac{|b_n(kr)|^2}{\sum_0^N \frac{2n+1}{4\pi}|b_n(kr)|^2}$.

The Proposed Method

The operational bandwidth of a spherical microphone array is defined by its upper and lower frequency limits. The lower frequency limit is bounded by sensor noise and other errors, such as a mismatch in microphone gain and phase response, inaccurate positioning of microphones and limited computational accuracy [29], that is not our concern in this paper. The upper frequency limit is bounded by spatial aliasing [24]. To avoid significant error due to spatial aliasing we must have $N \geq kr$ [24]. In fact, the upper frequency is determined by $k \leq N/r$. However, at a higher frequency, the performance of the microphone array degrades due to spatial aliasing. For example, in beamforming problem, because of spatial aliasing we are not able to compute $p_{nm}(k,r)$ precisely, and according to (19) we will have inaccurate beamforming which in turn, for instance, degrades DF in MD beamformer.

A. The Proposed Method for Maximum Directivity Beamformer

Recently, Alon and Rafaely proposed a beamforming method with aliasing cancellation and formulated it for some well-known beamformers such as maximum-directivity, maximum WNG, and minimum variance distortion less response (MVDR), which is called MDAC (maximum directivity with aliasing cancellation), MGAC (maximum WNG with aliasing cancellation), and MVDR-AC (MVDR with aliasing cancellation) respectively. In this section, first, we derive their MDAC beamformer from a different point of view (See Theorem 1). Then, based on our perspective we propose a new beamforming method with aliasing reduction to acquire better performance.

Theorem 1. The MDAC beam pattern is equivalent to the MD beam pattern corresponding to the minimum norm solution of (17).

Proof: In [1], Alon and Rafaely proved that the MDAC beam pattern is as

$$A_{MDAC}(k,\theta_k,\phi_k) = \tilde{\mathbf{w}}_{\mathbf{nm}}^{MD^{\boldsymbol{H}}}\mathbf{E}^H\left(\mathbf{E}\mathbf{E}^H\right)^{-1}\hat{\mathbf{v}}_{\mathbf{nm}} \tag{38}$$

where

$$\tilde{\mathbf{w}}_{\mathbf{nm}}^{MD} = \left[w_{00}(k), w_{1(-1)}(k), w_{10}(k), w_{11}(k)\ \ldots, w_{\tilde{N}\tilde{N}}(k)\right]^T \tag{39}$$

and $\hat{\mathbf{v}}_{\mathbf{nm}} = \mathbf{E}\tilde{\mathbf{v}}_{\mathbf{nm}}$, is the aliased version of

$$\tilde{\mathbf{v}}_{\mathbf{nm}} = \left[v_{00}(k,r), v_{1(-1)}(k,r), v_{10}(k,r), \ldots, v_{\tilde{N}\tilde{N}}(k,r)\ \right]^T \tag{40}$$

$w_{nm}(k)$ is as (33) and $v_{nm}(k,r)$ is as (29).

Now, we derive this result from a different point of view as follows. If we rewrite (17) for unit-amplitude plane wave we have

$$\hat{\mathbf{v}}_{\mathbf{nm}} = \mathbf{E}\tilde{\mathbf{v}}_{\mathbf{nm}} \tag{41}$$

It is an underdetermined linear equations, i.e., there are fewer equations than unknowns. Therefore, this equation has many solutions. The minimum norm solution of this equation is

$$\tilde{\mathbf{v}}_{\mathbf{nm}}^{\boldsymbol{min\_norm}} = \mathbf{E}^H\left(\mathbf{E}\mathbf{E}^H\right)^{-1}\hat{\mathbf{v}}_{\mathbf{nm}} \tag{42}$$

where $\mathbf{E}^H(\mathbf{E}\mathbf{E}^H)^{-1}$ is the pseudo-inverse of matrix $\mathbf{E}$.

Now, we have a plane wave, $\tilde{\mathbf{v}}_{\mathbf{nm}}^{\boldsymbol{min\_norm}}$, arriving from the direction (θ_k,ϕ_k), for which we can construct a beam pattern using beamforming coefficients $\tilde{\mathbf{w}}_{\mathbf{nm}}^{MD}$. Note that $\tilde{\mathbf{v}}_{\mathbf{nm}}^{\boldsymbol{min\_norm}}$ is an estimation of a unit-amplitude plane wave of order $\tilde{N}$. So, the beam pattern is as

$$\begin{aligned} A_{min\_norm}(k,\theta_k,\phi_k) &= \tilde{\mathbf{w}}_{\mathbf{nm}}^{MD^H}\tilde{\mathbf{v}}_{\mathbf{nm}}^{\boldsymbol{min\_norm}} \\ &= \tilde{\mathbf{w}}_{\mathbf{nm}}^{MD^{\boldsymbol{H}}}\mathbf{E}^H\left(\mathbf{E}\mathbf{E}^H\right)^{-1}\hat{\mathbf{v}}_{\mathbf{nm}} \end{aligned} \tag{43}$$

which is the same as $A_{MDAC}(k,\theta_k,\phi_k)$. □As we have mentioned before, (41) is an underdetermined linear equation and has many solutions. If we obtained the desired solution, $\tilde{\mathbf{v}}_{\mathbf{nm}}$, then by multiplying it with $\tilde{\mathbf{w}}_{\mathbf{nm}}^{MD^{\boldsymbol{H}}}$ we could obtain the best beamforming pattern, i.e. beam pattern with maximum directivity. So, in our proposed method, the aim is to find a solution as close as to $\tilde{\mathbf{v}}_{\mathbf{nm}}$. For that, we use the following theorem.

Theorem 2: The best beamforming pattern for maximum directivity beamformer can be obtained using $\tilde{\mathbf{v}}_{\mathbf{nm}}$ via solving the following optimization problem

$$\begin{aligned} &\underset{\tilde{\mathbf{v}}_{\mathbf{nm}}}{\text{minimize}}\ \|\mathbf{E}\tilde{\mathbf{v}}_{\mathbf{nm}} - \hat{\mathbf{v}}_{\mathbf{nm}}\| \\ &\text{subject to} \\ &\left|\sum_{\theta,\phi}\kappa_i^*(\theta,\phi)\kappa_j(\theta,\phi)\right| = 0, \forall i \neq j \\ &\left|\sum_{\theta,\phi}\kappa_i^*(\theta,\phi)\kappa_i(\theta,\phi)\right| = 1, \\ &(\theta,\phi) \in \{(\theta_1,\phi_1),(\theta_2,\phi_2),\ldots.,(\theta_Q,\phi_Q)\} \end{aligned} \tag{44}$$

where $\boldsymbol{\kappa}^* = \widetilde{\mathbf{B}}_D^{-1}\tilde{\mathbf{v}}_{\mathbf{nm}}$, and $\boldsymbol{\kappa} = [\kappa_1, \kappa_1, \dots, \kappa_{\widetilde{N}}]$. $\widetilde{\mathbf{B}}_D$ is as $\mathbf{B}_D$ in (30) with N replaced by $\widetilde{N}$ and (θ_i, ϕ_i), are the positions of the i^{th} sample.

Proof: We know that the spherical harmonics have orthogonality property [29], i.e,

$$\int_0^{2\pi}\int_0^{\pi}[Y_n^m(\theta,\phi)]^* Y_{n'}^{m'}(\theta,\phi)\sin\theta d\theta d\phi = \delta_{nn'}\delta_{mm'} \quad (45)$$

where $\delta_{nn'}$ is equal to unity for $n = n'$ and zero otherwise. Using this property as constraints, (41) can be solved using the following optimization problem

$$\begin{aligned} &\underset{\tilde{\mathbf{v}}_{\mathbf{nm}}}{\text{minimize}} \quad \|\mathbf{E}\tilde{\mathbf{v}}_{\mathbf{nm}} - \hat{\mathbf{v}}_{\mathbf{nm}}\| \\ &\text{subject to} \\ &\left|\int_0^{2\pi}\int_0^{\pi}\kappa_i^*(\theta,\phi)\,\kappa_j(\theta,\phi)\sin\theta\, d\theta\, d\phi\right| = 0 \\ &\qquad \forall i \neq j \\ &\left|\int_0^{2\pi}\int_0^{\pi}\kappa_i^*(\theta,\phi)\,\kappa_i(\theta,\phi)\sin\theta\, d\theta\, d\phi\right| = 1 \end{aligned} \quad (46)$$

where $\boldsymbol{\kappa}^*$ and $\widetilde{\mathbf{B}}_D$ is as defined above.

Considering the discrete form of these constraints results (44). Now, the MD beamforming with aliasing reduction is as follows

$$A_{MDAC_{Proposed}}(k,\theta_k,\phi_k) = \tilde{\mathbf{w}}_{\mathbf{nm}}^{MD^{\boldsymbol{H}}}\tilde{\mathbf{v}}_{\mathbf{nm}} \quad (47)$$

where $\tilde{\mathbf{v}}_{\mathbf{nm}}$ is the solution of (46).

B. The Proposed Method for Arbitrary Beamformer

We can apply the proposed method to an arbitrary beamformer as follows. First, we can solve the following optimization problem

$$\begin{aligned} &\underset{\tilde{\mathbf{p}}_{\mathbf{nm}}}{\text{minimize}} \quad \|\mathbf{E}\tilde{\mathbf{p}}_{\mathbf{nm}} - \hat{\mathbf{p}}_{\mathbf{nm}}\| \\ &\text{subject to} \\ &\left|\int_0^{2\pi}\int_0^{\pi}\kappa_i^*(\theta,\phi)\,\kappa_j(\theta,\phi)\sin\theta\, d\theta\, d\phi\right| = 0 \\ &\qquad \forall i \neq j \\ &\left|\int_0^{2\pi}\int_0^{\pi}\kappa_i^*(\theta,\phi)\,\kappa_i(\theta,\phi)\sin\theta\, d\theta\, d\phi\right| = 1 \end{aligned} \quad (48)$$

where $\boldsymbol{\kappa}^* = \widetilde{\mathbf{B}}_D^{-1}\tilde{\mathbf{p}}_{\mathbf{nm}}$. We assume that the solution to the above problem is $\tilde{\boldsymbol{\rho}}_{\boldsymbol{nm}}$. Then the desired beamforming with reduced aliasing is as follows

$$A_{proposed}(k,\theta_k,\phi_k) = \tilde{\mathbf{w}}_{\mathbf{nm}}^H\tilde{\boldsymbol{\rho}}_{\boldsymbol{nm}} \quad (49)$$

where $\tilde{\mathbf{w}}_{\mathbf{nm}}^H$ is the beamforming coefficients of the ordinary beamformer. For example, for maximum WNG beamformer $\tilde{\mathbf{w}}_{\mathbf{nm}}^H$ is as introduced in (36) with N replaced by $\widetilde{N}$.

Simulations Results

In this section we compare the proposed methods, MDAC$_{\text{Proposed}}$ and MGAC$_{\text{Proposed}}$, with counterparts in Alon and Rafaely's method, namely MDAC and MGAC. For this purpose, a microphone array with 50 microphones has been considered. These microphones are placed on the surface of a rigid sphere with radius of $r = 10$ cm, based on gaussian sampling scheme. The maximum order of an order-limited function that can be constructed from this configuration is $N = 4$ [29].

The operational bandwidth of this microphone array can be determined by the condition $kr \leq N$ which results $f_{max} = 2.1$ kHz. So, the array can not handle higher frequency without aliasing. The simulation is designed for three different frequencies, $k_1 r = 3.6$ ($\widetilde{N} = N = 4 > k_1 r$), $k_2 r = 8.1$ ($\widetilde{N} = 9 > k_2 r$), and $k_3 r = 14.2$ ($\widetilde{N} = 15 > k_3 r$) where each kr represents different frequency corresponds to $f_1 = 1.9$ kHz, $f_2 = 4.4$ kHz, and $f_3 = 7.6$ kHz.

A. MDAC$_{Proposed}$ Simulation

The look direction for every beamformer in this simulation is equal. The sound field around the sphere is composed of a single unit-amplitude plane wave of orders $\widetilde{N} = 4, 9, 15$ respectivly, and arrives from the same angle as look direction, $(\theta_0, \phi_0) = (\theta_l, \phi_l) = (90^\circ, 80^\circ)$. Beam patterns are compared over three different frequencies, $k_1 r = 3.6$, $k_2 r = 8.1$, and $k_3 r = 14.2$.

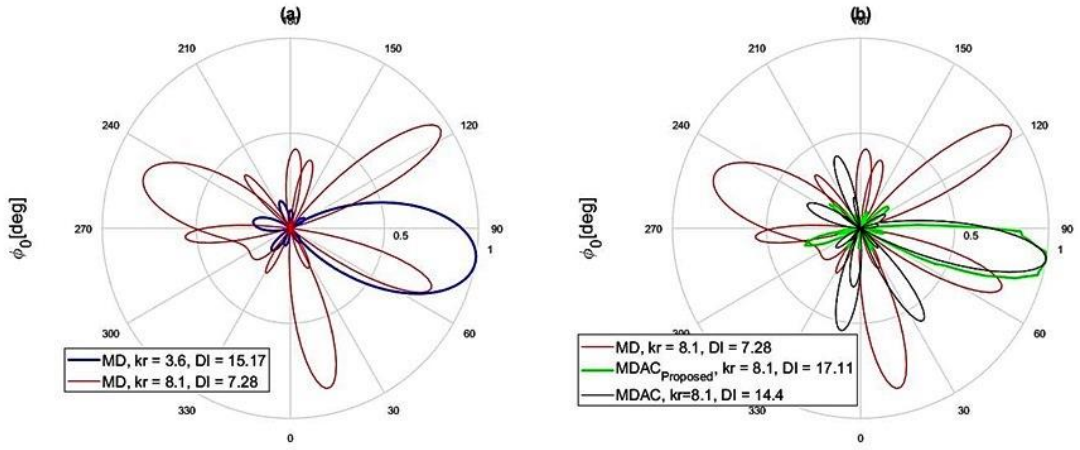

Fig. 1: The beam pattern of a fourth-order array with look direction $(\theta_l, \phi_l) = (90^\circ, 80^\circ)$ (a) comparison between MD beam patterns at frequencies $k_1 r = 3.6$ (f = 1.9 kHz) and $k_2 r = 8.1$ (f = 4.4 kHz) and (b) comparison between MD, MDAC$_{\text{Proposed}}$, and MDAC beamformers at $k_2 r = 8.1$ (f = 4.4 kHz).

Fig. 1(a) shows two beam patterns of MD beamformer at two different frequencies. At lower frequency, $k_1 r = 3.6$, a beam pattern is obtained for sound field of order $\widetilde{N} = 4$, so beamforming is done without any aliasing, however at a higher frequency, $k_2 r = 8.1$, side-lobe levels are increased and the beam pattern is not directional anymore. This performance degradation between $k_1 r$ and $k_2 r$ can be explained by the array's operational bandwidth. Here, the maximum frequency that can be handled by microphone array must be lower than $f_{max} = 2.1$ kHz as mentioned in the fourth section. Therefore, because of the $k_1 r \leq N$ ($f_1 \leq f_{max}$), aliasing free condition is satisfied and the array output is without aliasing. For the second part, because of the $k_2 r > N$, condition is not satisfied, and array response suffers from aliasing. Fig. 1(b) shows array beam patterns for three different beamformers (MD, MDAC, and MDAC$_{Proposed}$) in frequency of $k_2 r = 8.1$. The arrays performance for the MD beamformer is the same as part (a) of Fig. 1, but a comparison between MDAC and MDAC$_{Proposed}$ beam patterns shows that side-lobes are at much lower levels in MDAC$_{Proposed}$ than MDAC, in addition, main-lobe of MDAC$_{Proposed}$ is narrower than MDAC.

Another comparison between MD, MDAC, and MDAC$_{Proposed}$ beamformers is shown in Fig. 2, in which the plot balloon of these beamformers shows that MDAC$_{Proposed}$ has lower side-lobe levels compared to MDAC.

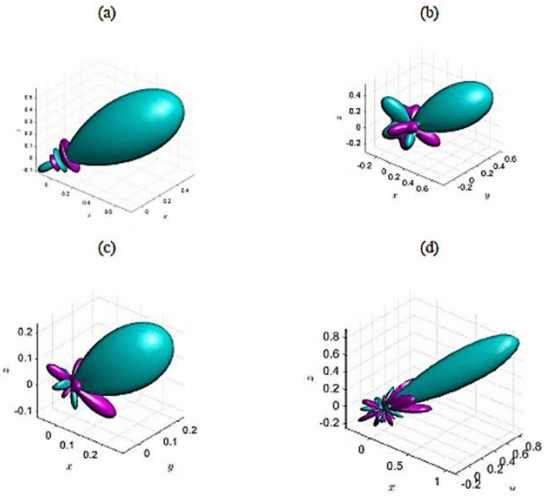

Fig. 2: Plot balloon comparison between MD, MDAC, and MDAC$_{Proposed}$ beamformers with look direction $(\theta_l, \phi_l) = (90^\circ, 80^\circ)$ (a) MD beamformer plot balloon at $k_1 r = 3.6$ ($f = 1.9$ kHz) (b) MD beamformer at $k_2 r = 8.1$ ($f = 4.4$ kHz) (c) MDAC beamformer at $k_2 r = 8.1$ ($f = 4.4$ kHz) (d) MDAC$_{Proposed}$ at $k_2 r = 8.1$ ($f = 4.4$ kHz).

A more computational manner for comparison between MD, MDAC, and MDAC$_{Proposed}$ beamformers is by comparing their directivity indexes calculated with (30). Table 1 shows the directivity index of each beamformer at $k_1 r$ and $k_2 r$. At $k_1 r = 3.6$, all beamformers used in this simulation have the same DI. The reason is that for each one the condition $kr \leq N$ is satisfied. However, at $k_2 r = 8.1$ the MDAC beamformer has DI $= 14.4$ but the DI for MDAC$_{Proposed}$ is 17.11. This shows that MDAC$_{Proposed}$ has improved directivity by nearly 19%.

Table 1: A comparison between DI of MD, MDAC, and MDAC$_{Proposed}$ beamformers in two different frequencies $k_1 r = 3.6$ and $k_2\, r = 8.1$

Beamformer	DI (dB) with $kr = 3.6$	DI (dB) with $kr = 8.1$
MD	13.9	7.28
MDAC	13.9	14.4
MDAC$_{Proposed}$	13.9	17.11

Fig. 3 shows a better comparison between MDAC and MDAC$_{Proposed}$ beamformers, where both are operating in the sound field with order of $\widetilde{N} = 15 > N$ and for $k_3 r = 14.2$ ($f_3 = 7.6$ kHz). In this figure, it is clear that MDAC beamformer has side-lobes of high levels, almost as high as the main-lobe, but the MDAC$_{Proposed}$ beamformer managed to keep the side-lobe levels as low as in $k_2 r$. This shows that the MDAC beamformer's performance decays as the sound field order increases but MDAC$_{Proposed}$ is robust enough to keep the side-lobe levels low. So, despite the low computational complexity in MDAC beamformer, the accuracy of this method decays when the frequency is extremely higher than f_{max}. In other words, when $kr \gg N$ it cannot perform well, but MDAC$_{Proposed}$ beamformer performed exactly as in $k_2 r = 8.1$. Because MDAC$_{Proposed}$ always uses a nearly optimum solution, the frequency does not affect its performance. In this case, MDAC$_{Proposed}$ improved DI by 42%, even higher improvement than it has at lower frequencies.

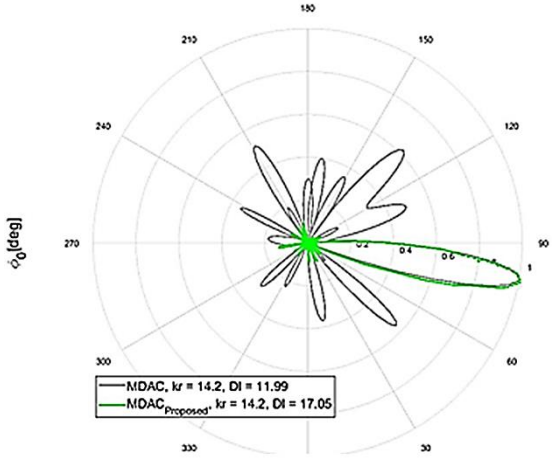

Fig. 3: A comparison between MDAC and MDAC$_{Proposed}$ beam patterns at the frequency $k_3 r = 14.2$ ($f_3 = 7.6$ kHz). The gray plot represents MDAC beam pattern with DI $= 11.99$ and green plot represents MDAC$_{Proposed}$ beam pattern with DI $= 17.05$.

B. MGAC$_{Proposed}$ Simulation

For this simulation, the same configuration as in the previous section for microphone array is used. Beamformers are compared at $k_1 r = 3.6$ and $k_2 r = 8.1$ which represent frequencies of $f_1 = 1.9\,\text{kHz}$ and $f_2 = 4.4\,\text{kHz}$ respectively. Table 2 shows the WNG of maximum WNG beamformer (MG), MGAC, and MGAC$_{\text{Proposed}}$ beamformers. As it shows, all of the beamformers attained the WNG of 15.8 at $k_1 r$. This is because of the fact that the condition $kr < N$ is satisfied at $k_1 r = 3.1$. But in $k_2 r = 8.1$ the WNG drops for MG beamformer due to the beamformer's bandwidth limitation. It can be seen that WNG is improved by nearly 15% in MGAC$_{\text{Proposed}}$ compared to MGAC beamformer.

For more comparison between MGAC and MGAC$_{\text{Propsed}}$ beamformers, Table 3 shows DI of these two beamformers at frequencies $k_1 r$ and $k_2 r$ in which it can be seen that MGAC$_{\text{Propseed}}$ improved DI by 3%. Although this is not a major improvement, it should be noted that improving WNG does not necessarily improve DI [30], but it is worthwhile to note that while improving the WNG, MGAC$_{\text{Proposed}}$ also improved DI.

Table 2: A comparison between WNG of MG, MGAC, and MGAC$_{\text{Proposed}}$ beamformers in two different frequencies $k_1 r = 3.6$ and $k_2\, r = 8.1$

Beamformer	WNG with $kr = 3.6$	WNG with $kr = 8.1$
MG	15.8	10.93
MGAC	15.8	15.91
MGAC$_{\text{Proposed}}$	15.8	16.54

Table 3: A comparison between DI of MG, MGAC, and MGAC$_{\text{Proposed}}$ beamformers in two different frequencies $k_1 r = 3.6$ and $k_2\, r = 8.1$

Beamformer	DI (dB) with $kr = 3.6$	DI (dB) with $kr = 8.1$
MG	12.3	8.71
MGAC	12.3	13.7
MGAC$_{\text{Proposed}}$	12.3	14.21

Results and Discussion

The simulation results show that the proposed method has the ability to extend the operational bandwidth of a spherical microphone array and consequently achieves higher DI and lower side lobe level compared to MDAC and MD beamformers in high frequencies. In addition to the MDAC beamformer, this method can be extended to other beamforming methods such as maximum WNG beamformer. Simulation results show improvement over those beamformers as well.

Conclusion

Aliasing and, in consequence, unwanted side lobe formation is the main factor in spherical microphone arrays operational bandwidth determination. Most of the methods previously presented to reduce aliasing demanded physical changes in the array structure which comes at a cost.

Recently Alon and Rafely presented a method to reduce aliasing in high frequencies without demanding a physical change in array. This method is based on including the effect of spatial aliasing in the definition of desired objective. Their approach found to be useful in developing aliasing cancellation capability for beamformers. In this paper we proposed a new method based on Alon and Rafaely's approach via designing a constrained optimization problem using orthogonality property of spherical harmonics, to achieve better performance.

The proposed method achieves higher DI and lower side lobe level compared to MDAC and MD beamformers in high frequencies and results show that it has improved the MDAC beamformer performance by nearly 19%. In addition to the MDAC beamformer, this method can be extended to other beamforming methods such as maximum WNG beamformer. Simulation results show improvement of WNG by nearly 15% over MGAC beamformer.

Because the optimization problem in this method can be of very high dimension, obtaining the unaliased signal can be time consuming. Thus, the presented method cannot be applied to real time purposes. For future work it can be considered to develop this approach for real time applications. Also, the derivation of formula in this work is based on the plane wave assumption for arriving waves.

So, we assume implicitly far field waves in our proposed method. Aliasing cancellation beamformer for near field sound waves is also suggested for future work.

Author Contributions

M. Kalantari proposed the method. M. Kalantari and M. Mohammadpour Tuyserkani implemented the proposed method, interpreted the results and wrote the manuscript. Solving the optimization problems carried out by S. H. Amiri. He also contributed in writing the manuscript.

Acknowledgments

This work was supported by Shahid Rajaee Teacher Training University under contract number 15947.

Conflict of Interest

The authors declare no potential conflict of interest regarding the publication of this work. In addition, the ethical issues including plagiarism, informed consent, misconduct, data fabrication and, or falsification, double publication and, or submission, and redundancy have been completely witnessed by the authors.

Abbreviations

MVDR	Minimum variance distortionless response
MD	Maximum directivity
MG	Maximum white noise gain
DI	Directivity index
MDAC	Maximum directivity beamformer with aliasing cancellation
MGAC	Maximum white noise gain beamformer with aliasing cancellation
MVDR-AC	Minimum variance distortionless response with aliasing cancellation
SNR	Signal-to-noise ratio
WNG	White noise gain
α_q	Sampling weights
$\boldsymbol{\alpha}$	Vector of sampling weights
θ	Elevation angle
ϕ	Azimuth angle
$a(\cdot)$	Plane-wave decomposition in the space domain
a_{nm}	Plane-wave decomposition in the spherical-harmonics domain
$b_n(\cdot)$	Function relating pressure to plane-wave decomposition
DF	Directivity factor
d_n	Axis-symmetric beamforming weighting function
$j_n(\cdot)$	Spherical Bessel function of the first kind
k	Wave number
$\mathbf{k}$	Wave vector denoting propagation direction
$\tilde{\mathbf{k}}$	Wave vector denoting arrival direction
N	Order of spherical harmonics
p	Sound pressure in the space domain
p_{nm}	Sound pressure in the spherical harmonics domain
$\mathbf{p}$	Sound pressure vector in the space domain
$\mathbf{p_{nm}}$	Sound pressure vector in the spherical harmonics domain
Q	Number of samples or microphones
$\mathbf{r}$	Vector of spherical coordinates
$\mathbf{v}$	Steering vector in the space domain
$\mathbf{v_{nm}}$	Steering vector in the spherical harmonics domain
$w(\cdot)$	Beamforming weighting function in the space domain
w_{nm}	Beamforming weighting function in the spherical harmonics domain
$\mathbf{w}$	Beamforming weighting vector in the space domain
$\mathbf{w_{nm}}$	Beamforming weighting vector in the spherical harmonics domain
$Y_n^m(\cdot)$	Spherical harmonics
$\mathbf{Y}$	Matrix of Spherical harmonics

References

[1] D. Alon, B. Rafaely, "Beamforming with optimal aliasing cancellation in spherical microphone arrays," IEEE/ACM Trans. Audio Speech Lang. Process., 24(1): 196-210 2016.

[2] B. Bernschütz, "Bandwidth extension for microphone arrays," in Proc. 133th AES Convention, San Francisco, USA: 1–10, 2012.

[3] B. Bernschütz, "Microphone arrays and sound field decomposition for dynamic binaural recording", Ph.D. thesis, Technische Universität Berlin, 2016.

[4] W.H. Liao, Y. Mitsufuji, K. Osako, K. Ohkuri, "Microphone array geometry for two dimensional broadband sound field recording," in Proc. Audio Engineering Society Convention, 2018.

[5] T.D. Abhayapala, D.B. Ward, "Theory and design of high order sound field microphones using spherical microphone array," in Proc. ICASSP: 1949–1952, 2002.

[6] B. Rafaely, "Spatial sampling and beamforming for spherical microphone arrays," in Proc. Hands-Free Speech Communication and Microphone Arrays (HSCMA): 5-8, 2008.

[7] J. Meyer, G. Elko, "A highly scalable spherical microphone array based on an orthonormal decomposition of the sound field", in Proc. IEE Int. Conf. Acoustics, Speech, and Signal Processing (ICASSP): II–1781–II–1784, 2002.

[8] Z. Li, R. Duraiswami, "Flexible and optimal design of spherical microphone arrays for beamforming," IEEE Trans. Audio Speech Lang. Process., 15(2): 702–714, 2007.

[9] H. Beit-On, B. Rafaely, "Focusing and frequency smoothing for arbitrary arrays with application to speaker localization," IEEE/ACM Trans. Audio Speech Lang. Process., 28: 2184-2193, 2020.

[10] M.R.P. Thomas, "Practical concentric open sphere cardioid microphone array design for higher order sound field capture," in Proc. ICASSP-IEEE International Conf. Acoustics, Speech and Signal Processing (ICASSP): 666-670, 2019.

[11] D.P. Jarret, E.A.P. Habets, P.A. Naylor, Theory and Applications of Spherical Microphone Array Processing, Springer, 2017.

[12] B. Rafaely, "Plane-Wave decomposition of the sound field on a sphere by spherical convolution," J. Acous. Soc. Am., 116(4): 2149–2157, 2004.

[13] V. Pulkki, S. Delikaris-Manias, A. Politis, "Spatial decomposition by spherical array processing," in Proc. Parametric Time-Frequency Domain Spatial Audio, IEEE: 25-47, 2018.

[14] J. R. Driscoll, D. M. Healy, "Computing Fourier transforms and convolutions on the 2-sphere," Adv. Appl. Math., 15(2): 202–250, 1994.

[15] A.H. Moore, M. Brookes, P.A. Naylor, "Robust spherical harmonic domain interpolation of spatially sampled array manifolds," in Proc. IEEE International Conf. Acoustics, Speech and Signal Processing (ICASSP), 2017.

[16] B. Rafaely, "Analysis and design of spherical microphone arrays," IEEE Trans. Speech Audio Process., 13(1): 135–143, 2005.

[17] U. Elahi, Z. Khalid, R.A. Kennedy, "Design of a spatially constrained anti-aliasing filter using slepian functions on the sphere," in Proc.

13th International Conf. Signal Processing and Communication Systems (ICSPCS): 1-6, 2019.

[18] B. Bernschutz, "Bandwidth extension for microphone arrays", in Proc. Audio Engineering Society Convention 133, Audio Engineering Society, 2012.

[19] U. Elahi, Z. Khalid, R.A. Kennedy, "Spatially constrained anti-aliasing filter using slepian eigenfunction window on the sphere," in Proc. 12th International Conf. Signal Processing and Communication Systems (ICSPCS): 1-6, 2018.

[20] J. Lin, X. Wu, T. Qu, "Anti spatial aliasing HOA encoding method based on aliasing projection matrix," in Proc. IEEE 3rd International Conf. Information Communication and Signal Processing (ICICSP): 321-325, 2020.

[21] J. Dmochowski, J. Benesty, S. Affes, "On spatial aliasing in microphone arrays," IEEE Trans. Signal Process., 57(4): 1383–1395, 2009.

[22] X. Zhao, G. Huang, J. Chen, J. Benesty, "An improved solution to the frequency-invariant beamforming with concentric circular microphone arrays," in Proc. IEEE International Conf. Acoustics, Speech and Signal Processing (ICASSP): 556-560, 2020.

[23] A. Macovski, "Ultrasonic imaging using arrays," in Proc. IEEE, 67(4): 484–495, 1979.

[24] B. Rafaely, B. Weiss, E. Bachmat, "Spatial aliasing in spherical microphone arrays," IEEE Trans. Signal Process., 55(3): 1003–1010, 2007.

[25] M. Agmon, B. Rafaely, J. Tabrikian, "Maximum directivity beamformer for spherical-aperture microphones," in Proc. IEEE Workshop on Applications of Signal Processing to Audio and Acoustics (WASPAA): 153–156, 2009.

[26] V. Tourbabin, B. Rafaely, "Sub-Nyquist spatial sampling using arrays of directional microphones," in Proc. Joint Workshop on Hands-free Speech Communication and Microphone Arrays (HSCMA): 76–80, 2011.

[27] S. Brown, V. Sethu, D. Taubman, "Spatial wiener filter to reduce spatial aliasing with spherical microphone arrays," J. Acous. Soc. Am., 145(4): 2254-2264, 2019.

[28] A.D. Firoozabadi, P. Irarrazaval, P. Adasme, H. Durney, M.S. Olave, "A novel quasi-spherical nested microphone array and multiresolution modified SRP by gammatone filterbank for multiple speakers localization," in Proc. Signal Process.: Algorithms, Architectures, Arrangements, and Applications (SPA): 208-213 2019.

[29] B. Rafaely, Fundamentals of Spherical Arrays Processing, Springer, 2nd edn., 2018.

[30] B. Rafaely, "Phase-Mode versus delay-and-sum spherical microphone array processing," IEEE Signal Process. Lett., 12(10): 713–716, 2005.

Biography

Mohammad Kalantari received B.Sc. degree in Computer Engineering from Iran University of Science and Technology (IUST), Tehran, Iran and M.Sc. and Ph.D. in Computer Engineering from Amirkabir University of Technology (AUT), Tehran, Iran in 2001 and 2009 respectively. He is currently working as Assistant Professor at Signal Processing Laboratory in Computer Engineering Department at Shahid Rajaee Teacher Training University (SRTTU), Tehran, Iran. His area of interest includes, statistical signal processing, spherical array processing, sampling theory and compressed sensing.

- Email: mkalantari@sru.ac.ir
- ORCID: 0000-0002-6852-9344
- Web of Science Researcher ID: NA
- Scopus Author ID: 55893680300
- Homepage: https://www.sru.ac.ir/kalantari/

Mohammadmehdi Mohammadpour Tuyserkani received B.Sc. degree in Computer Engineering from Shahed University, Tehran, Iran in 2016. He is currently working as a Research Assistant in Signal Processing Laboratory in the faculty of Computer Engineering at Shahid Rajaee Teacher Training University (SRTTU), Tehran, Iran. His area of interest includes spherical array processing, statistical signal processing and machine learning.

- Email: mm.mohammadpour@sru.ac.ir
- ORCID: NA
- Web of Science Researcher ID: NA
- Scopus Author ID: NA
- Homepage: NA

Seyed Hamid Amiri received B.Sc. degree in Software Engineering from Shahid Bahonar University, Kerman, Iran and M.Sc. and Ph.D. in Artificial Intelligence from Sharif University of Technology (SUT), Tehran, Iran in 2009 and 2015 respectively. He is currently working as Assistant Professor in Computer Engineering Department at Shahid Rajaee Teacher Training University. His area of interest includes computer vision and video processing, statistical signal processing, statistical pattern recognition and numerical optimization in artificial intelligence.

- Email: s.hamidamiri@sru.ac.ir
- ORCID: 0000-0002-4723-896X
- Web of Science Researcher ID: NA
- Scopus Author ID: 57197243231
- Homepage: https://www.sru.ac.ir/hamidamiri/

How to cite this paper:

M. Kalantari, M. Mohammadpour Tuyserkani, S.H. Amiri, "A general approach for operational bandwidth extension in spherical microphone array," J. Electr. Comput. Eng. Innovations, 10(2): 393-402, 2022.

DOI: 10.22061/JECEI.2021.8304.501

URL: https://jecei.sru.ac.ir/article_1680.html